Modeling and Analysis of an Innovative Waste Heat Recovery System for Helicopters

Georgios C. Christidis[1], Ioannis Ch. Karatzaferis[1], Matthieu Sautreuil[2], Emmanuel C. Tatakis[1], Nikolaos P. Papanikolaou[3]

[1]UNIVERSITY OF PATRAS
Laboratory of Electromechanical Energy Conversion
Electrical and Computer Engineering Department
26504, Rion-Patras, Greece
Tel.: +30.2610.996414
E-Mails: gchristidis@ece.upatras.gr, jkaratzaferis@ece.upatras.gr, e.c.tatakis@ece.upatras.gr
URL: http://lemec.ece.upatras.gr

[2]EADS-EUROCOPTER
Marignane, France
E-mail: Matthieu.Sautreuil@eurocopter.com

[3]TECHNOLOGICAL EDUCATIONAL INSTITUTE OF LAMIA
Department of Electrical Engineering
Lamia, 35100, Greece
Tel.: +30.22310.60254
E-Mail: npapanikolaou@teilam.gr
URL: http://www.teilam.gr

Acknowledgements

This research is being conducted in the frame of Cleansky JTI Project (RENERGISE no. 287076), a FP7 European Integrated project – http://www.cleansky.eu

Keywords

Energy savings, aerospace, control methods for energy systems, modeling, regenerative power, thermoelectric energy, simulation, AC machine, active filter, DC grid, supercapacitor

Abstract

The efficiency of helicopters is limited due to the high power losses of combustion engines, a fraction of which can be recovered and provided to the electrical bus by exploiting the heat found in the exhaust gases and through power electronics converters. The first system recovers energy through a thermoelectric generator, whereas the second through a permanent magnet generator rotated by a steam turbine. A third power converter, connected to a supercapacitor bank, compensates the peak currents demanded by the loads. Since extensive simulations have to be run in order to validate the feasibility of those systems, average models of the power converters are derived, and their accuracy is examined. Finally, based on those average models, the developed control strategy is examined.

Introduction

Within the scope of the "More electric aircraft" [1], more and more mechanical and hydraulic systems found in airplanes and helicopters are converted to electrical ones in order to save weight and to maximize efficiency and reliability. Therefore, the aircraft's power supply has to be able to take up those new growing load demands, without diminishing the power quality supplied to existing loads. Moreover, due to the augmented price of fuel, as well as for environmental reasons, a lot of research is targeted into increasing the efficiency of those high power consuming systems. Hence, the power losses of combustion engines continue to be greater than the energy provided, and as a result, it is essential to try and exploit those great amounts of power in the form of heat and convert them to usable energy.

In this paper, two waste heat energy recovery systems are presented, suitable for newly developed helicopters, which take advantage of the energy found in exhaust gases. This heat is converted into electrical energy and with special power electronics converters, is injected to the helicopter electrical dc grid [2].

The first system (called static waste heat recovery system – SWHR as it has no moving parts), depicted in fig. 1, uses thermoelectric generators [3], which are semiconductor devices that convert a temperature difference between two sides into an electrical voltage. Afterwards, there is a unidirectional voltage step-up boost converter, of 1kW nominal power, which connects the generator to the dc bus. What is more, there is a second converter, a voltage step-up/step-down buck/boost bidirectional converter, whose role is to supply and absorb the peak power generated by certain loads during transients. The energy is stored in a supercapacitor bank, which is selected because of the extremely high power density it provides [4]-[5]. This converter is necessary in order to smooth the current supplied by the helicopter main generator so as to increase its reliability and diminish the voltage fluctuation of the dc bus.

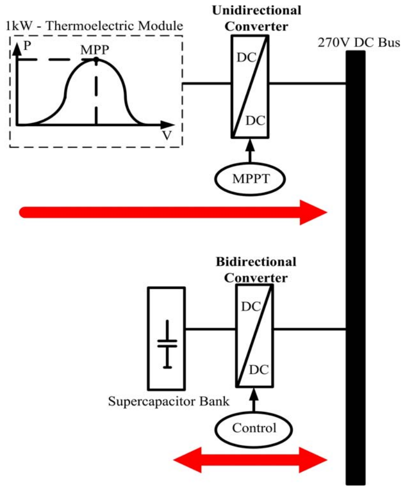

Fig. 1: Static Waste Heat Recovery System

The second system (called dynamic waste heat recovery system – DWHR), shown in fig. 2 employs a turbine, rotated using steam that is generated by a boiler placed at the engine nozzle. This turbine is connected to a permanent magnet synchronous generator (PMG), which supplies the energy to the dc bus through a power electronics converter, whose nominal power is 30kW. Due to the PMG high line frequency (around 2500Hz) and the high output power level, the topology used for the converter is a square wave, line commutated inverter, operating in a rectifying mode (energy flow from the AC side to the DC side). The desired output power is set by controlling the delay of the inverter voltage, which is the generator stator voltage, relatively to the generator emf voltage which is measured with the use of a position resolver. More information about the selection criteria of the above converters due to the special working conditions (high temperature, high altitude, vibrations) as well as the specific requirements of helicopter (low mass and volume) can be found in [2].

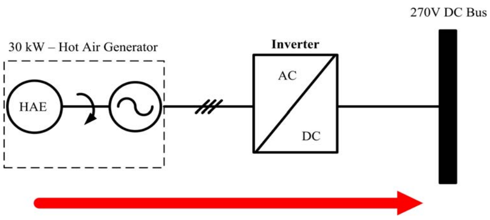

Fig. 2: Dynamic Waste Heat Recovery System

Due to the complexity of the systems presented and because of the extensive tests that they have to pass through, before being tested in real helicopters, the simulation analysis is essential in order to validate the feasibility of such a solution and examine the effect that it will have to the whole electrical network. Even so, if normal switching models of the converters are used, it is impossible to monitor the behavior of the system because of the enormous simulation times needed. On the other hand, average (functional) models can rapidly decrease simulation complexity, guaranteeing however, that they provide an accurate presentation of the system. In the following sections a presentation of the average models developed for those systems will be shown, as well as the control that has to be employed, followed by indicative simulation results.

Average Model Derivation

As power electronics converters are nonlinear systems, the simulation programs need to numerically solve a large amount of equations taking a lot of time. Therefore, behavioral models are used to evaluate the steady state operation and the response during a fast transient. In order to assess the behavior of the addition of those converters to a large and complex system, they need to be averaged and linearized.

For this reason two different approaches of functional modeling have been developed; the circuit-averaging technique [6]-[8], which transforms power electronics converters into a circuit of voltage and current sources, controlled by the duty cycle and the state-space averaging technique [9]-[11], which uses the equations that are derived by analyzing the equivalent linear circuits for the different subcircuits which exist when the switches are on or off. These equations are weighted, according to the duty cycle. Each technique has its own advantages. The circuit averaging method can easily include parasitic elements and converter losses. Moreover, the models are derived by examining the elements of the designed converter or device. On the other hand, the state-space averaging technique is good to verify the stability of the designed control. Based on the application and the requirements of the computer simulation, either one or both techniques can be implemented in order to be able to validate the operation of the electrical equipment.

The circuit averaging technique has been used to generate the average models of the converters of the SWHR system, including power losses, whereas the state space averaging technique was used to generate the average model of the DWHR.

Boost and Buck Converter

For the power loss analysis, it should be noted that only conduction losses are taken into account, since switching losses are a function of the switching frequency and for the derivation of the average models, the switching frequency is not taken into account. The switching losses could be included as well by a correction factor to the ohmic resistances of the converter elements. Both converters operate in Continuous Conduction Mode (CCM).

Fig.3 shows the switching and the average model of a boost converter, taking conduction power losses into account. The boost converter model is applied for the unidirectional SWHR converter, as well as the bidirectional SWHR converter when it supplies power, whereas the buck model is applied for the bidirectional SWHR converter when it absorbs power from the dc bus. Depending on the circuit conditions, switches manage the transition between the circuits.

According to the circuit averaging technique, the controlled switch is transformed into a controlled current source, whereas the diode is transformed into a controlled voltage source.

$$i_{SW} = \delta \cdot i_L \tag{1}$$

$$V_D = \delta \cdot V_o \tag{2}$$

where δ is the duty cycle of the converter and V_o the output voltage.
What is more, the conduction losses of the inductor (as an ohmic resistance), the power switch (as an ohmic resistance), the diode (as an ohmic resistance and a voltage drop) and the output capacitor (as

an ohmic resistance) are also included. The first three ohmic resistances are connected in series to the inductor for simulation convergence reasons. These resistances are determined based on the fact that the power losses of the two circuits must be equal.
For the inductor:

$$P_{Lb}' = P_{Lb} \Rightarrow i_L^2 \cdot R_{Lb}' = i_L^2 \cdot R_{Lb} \Rightarrow R_{Lb}' = R_{Lb} \tag{3}$$

For the controlled switch:
The RMS value of the current of the switch is [12]:

$$i_{SW,RMS} = i_L \cdot \sqrt{\delta} \tag{4}$$

So:

$$P_{SW}' = P_{SW} \Rightarrow i_L^2 \cdot R_{SW}' = i_{SW,RMS}^2 \cdot R_{SW} \Rightarrow i_L^2 \cdot R_{SW}' = \left(\sqrt{\delta} \cdot i_L\right)^2 \cdot R_{SW} \Rightarrow R_{SW}' = \delta \cdot R_{SW} \tag{5}$$

For the power diode:
The RMS value of the current of the diode is:

$$i_{D,RMS} = i_L \cdot \sqrt{1-\delta} \tag{6}$$

So:

$$P_D' = P_D \Rightarrow i_L^2 \cdot R_D' + i_D \cdot V_f = i_{D,RMS}^2 \cdot R_D + i_D \cdot V_f \Rightarrow i_L^2 \cdot R_D' = \left[\sqrt{1-\delta} \cdot i_L\right]^2 \cdot R_D \Rightarrow R_D' = (1-\delta) \cdot R_D \tag{7}$$

Finally, for the output capacitor:

$$P_{Co}' = P_{Co} \Rightarrow i_{Co}^2 \cdot R_{Co}' = i_{Co}^2 \cdot R_{Co} \Rightarrow R_{Co}' = R_{Co} \tag{8}$$

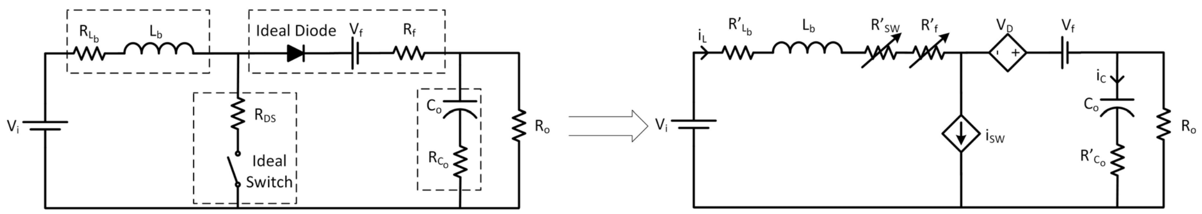

Fig. 3: Switching (behavioral) and average (functional) model of a boost converter

Fig. 4 shows the switching and the average model of the buck converter. The same principles as previously are considered. The controlled switch is transformed into a controlled current source, whereas the diode is transformed into a controlled voltage source:

$$i_{SW} = \delta \cdot i_L \tag{9}$$

$$V_D = \delta \cdot V_i \tag{10}$$

Then, by equating the power losses of the two circuits:
For the inductor:

$$P_{Lb}' = P_{Lb} \Rightarrow i_L^2 \cdot R_{Lb}' = i_L^2 \cdot R_{Lb} \Rightarrow R_{Lb}' = R_{Lb} \tag{11}$$

For the controlled switch:
The RMS value of the current of the switch is:

$$i_{SW,RMS} = i_L \cdot \sqrt{\delta} \tag{12}$$

So:

$$P_{SW}' = P_{SW} \Rightarrow i_L^2 \cdot R_{SW}' = i_{SW,RMS}^2 \cdot R_{SW} \Rightarrow i_L^2 \cdot R_{SW}' = \left(\sqrt{\delta} \cdot i_L\right)^2 \cdot R_{SW} \Rightarrow R_{SW}' = \delta \cdot R_{SW} \tag{13}$$

For the power diode:
The RMS value of the current of the diode is:

$$i_{D,RMS} = i_L \cdot \sqrt{1-\delta} \tag{14}$$

So:

$$P_D' = P_D \Rightarrow i_L^2 \cdot R_D' + i_D \cdot V_f = i_{D,RMS}^2 \cdot R_D + i_D \cdot V_f \Rightarrow i_L^2 \cdot R_D' = \left[\sqrt{1-\delta} \cdot i_L\right]^2 \cdot R_D \Rightarrow R_D' = (1-\delta) \cdot R_D \tag{15}$$

Finally, for the output capacitor:

$$P_{Co}' = P_{Co} \Rightarrow i_{Co}^2 \cdot R_{Co}' = i_{Co}^2 \cdot R_{Co} \Rightarrow R_{Co}' = R_{Co} \tag{16}$$

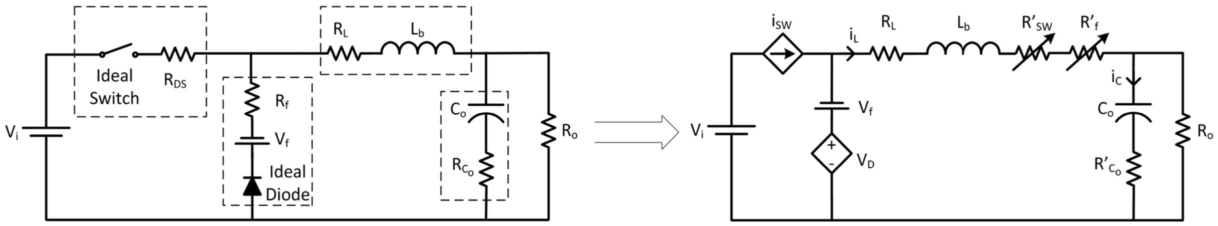

Fig. 4: Switching (behavioral) and average (functional) model of a buck converter

Square wave inverter, operating in rectifying mode

For the DWHR converter, the state-space average value model has been used [13]-[16].
As mentioned before, the power flow is set by controlling the delay of the inverter voltage relatively to the generator emf voltage. Since energy flow is required from the generator to the inverter, the inverter voltage should be delayed relatively to the generator. This can be seen in fig. 6, where the generator emf, inverter phase voltage and current are presented. The same principle is demonstrated in fig. 7, where the corresponding vector diagram is presented.

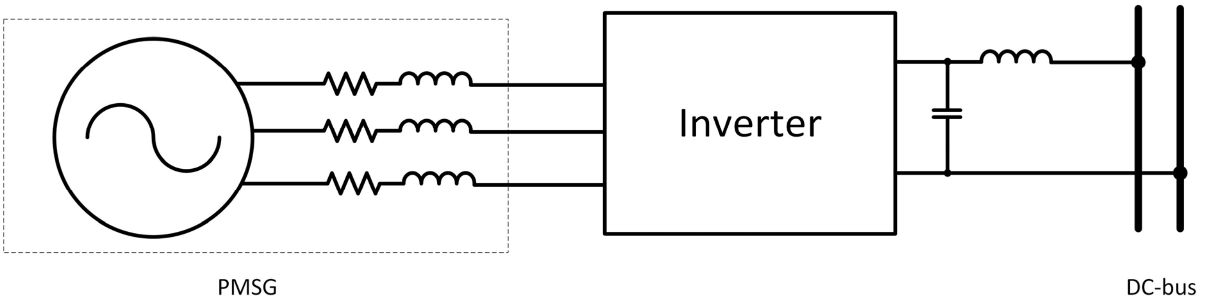

Fig. 5: The Dynamic waste heat recovery system

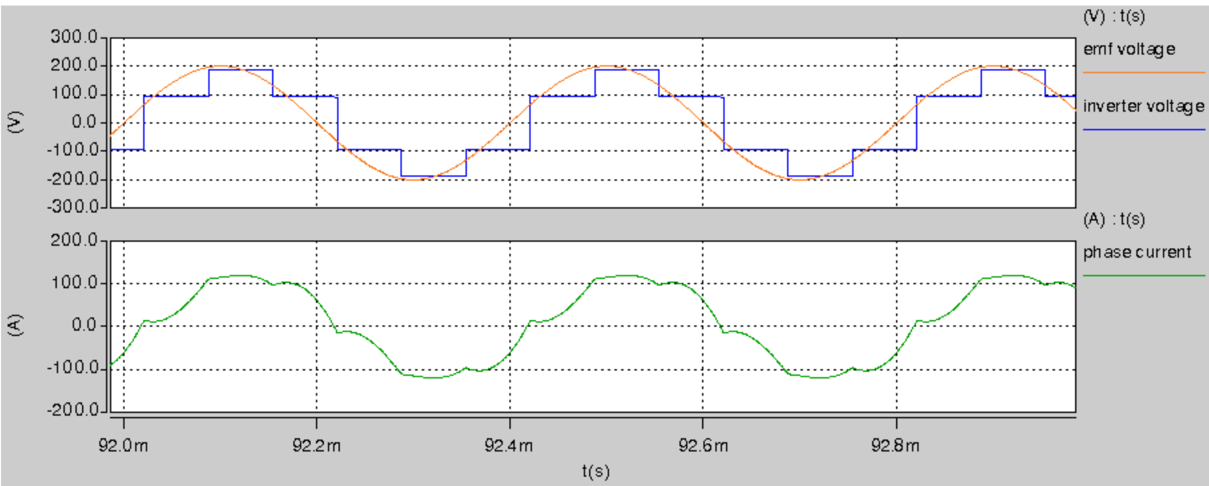

Fig. 6: Generator emf voltage and inverter phase voltage (upper case) and the resulting line current (lower case)

The AC-side voltage of the converter has to be transformed into dq reference frame, rotating with the generator's rotor speed. This leads to constant q and d axis voltages, which is required in order to result to the final state-space equations. Only the fundamental component of the inverter voltage is being considered, since the higher order components do not create active power.
Considering the above:

$$v_{qs} = k \cdot Vdc \cdot \cos a \quad (17)$$

$$v_{ds} = k \cdot Vdc \cdot \sin a \quad (18)$$

Where $k = \frac{v_{inverter,rms}}{Vdc}$ is the ratio of the fundamental voltage component to the dc bus voltage and α is the delay angle.

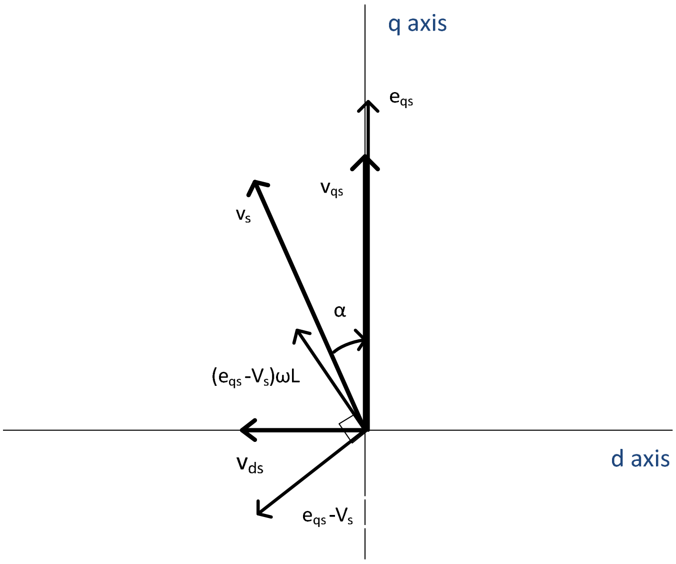

Fig. 7: Corresponding to the aforementioned analysis vector diagram.

Having the quantities v_{qs} and v_{ds} defined, we can now proceed to the average model state–space equations:

$$\frac{di_{qs}}{dt} = \frac{e_{qs}}{L_s} - \frac{R_s}{L_s} i_{qs} - \frac{k \cdot Vdc \cdot \cos a}{L_s} - \omega i_{ds} \quad (19)$$

$$\frac{di_{ds}}{dt} = \frac{e_{ds}}{L_s} - \frac{R_s}{L_s} i_{ds} - \frac{k \cdot Vdc \cdot \cos a}{L_s} + \omega i_{qs} \quad (20)$$

$$I_{dc} = -\frac{3}{2} \cdot k \cdot \sin a \cdot I_q + \frac{3}{2} \cdot k \cdot \cos a \cdot I_d \quad (21)$$

A block diagram of the average (functional) model for the DWHR converter can be seen in fig. 8.

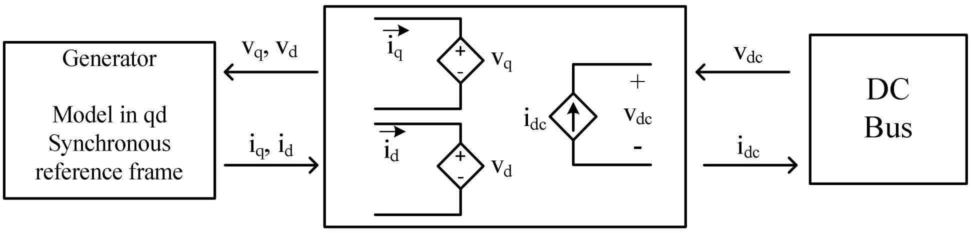

Fig. 8: Average (functional) model of a square wave inverter

Control of the Waste Heat Recovery System

Having developed those average models, extensive simulations, which will evaluate the operation of the converters as well as the network stability, can be carried out. While the first SWHR converter needs to supply a constant power, provided by the thermoelectric generator, the second converter has to detect transient load current changes and provide the power, in order for the main generator current to remain as constant as possible, and for the DC bus voltage fluctuation to remain as low as possible. What is more, during step load changes, the power supplied by the DWHR system should also be changed smoothly, in order to avoid high rates of torque increment or decrement for the generator. This is a requirement imposed by the hot air turbine that rotates the PMG.

 ISBN: 978-90-75815-17-7 and 978-1-4799-0114-2

Based on the above requirements, the control strategy is developed. The SWHR unidirectional boost converter operates as a current source and a Maximum Power Point Tracking (MPPT) algorithm has to be implemented, in order to harvest the maximum available power provided by the Thermoelectric Generator [17].

The aim of the DWHR system and the bidirectional buck/boost converter is to compensate the current transients demanded by the load, in order for the current of the main generator to fluctuate as little as possible. The DWHR system operates as a controlled current source that supplies the transient loads current, as long as the required power is within its nominal power. However, the power supplied by the DWHR system should change smoothly, as mentioned above. Therefore, the bidirectional converter also operates as a current source, supplying or absorbing the fast transient currents that cannot be supplied by the DWHR system. This energy is provided by the supercapacitor bank. Therefore, under normal conditions (when there is no transient load), its voltage remains constant. However, when extra power is needed in order to compensate the transient load, it is provided by the supercapacitor bank, which results to a decrease of its voltage. When the transient current is over, the capacitor is gradually recharged to its original voltage by the DC bus. To implement the above, the hysteresis current control for the inductor current of the buck/boost converter was selected. The current reference is the transient load current multiplied by the voltage ratio of the dc bus divided by the supercapacitor voltage. When there is a large deviation from the supercapacitor reference voltage, the supercapacitor is gradually charged or discharged to the reference voltage via a PI controller.

Simulation Results

The waste heat recovery system was simulated in SABER [18], in order to compare the average models generated to the switching ones and to examine and optimize the developed system.

The operation of the SWHR bidirectional converter during a fast transient load (boost operation) is depicted in fig. 9, both for the switching (behavioral) model and for the average (functional) one, whereas fig. 10 shows both models for a slow transient (buck operation). Both figures have the same scales. First of all, the consistency of the average model is observed, as the difference of between the waveforms of the average model and the switching models are minimal. Moreover, the fluctuation of the current drawn by the dc bus main generator is limited, proving the advantage of employing such a system. More specifically, the generator current is reduced to 12.5% and 10% in fig. 9 and fig. 10 respectively.

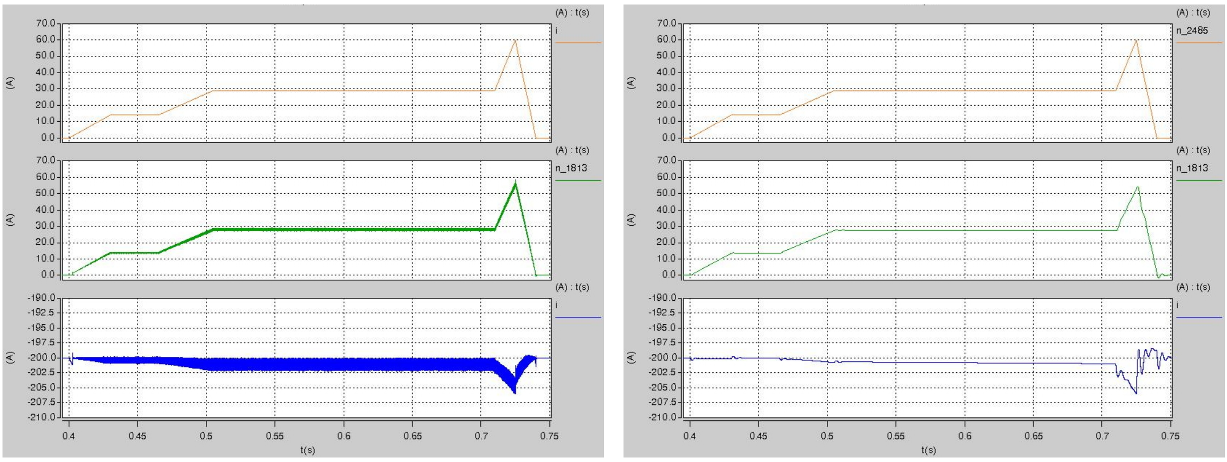

(a) (b)

Fig. 9: From top to bottom: transient current, converter output current and main generator current for switching (behavioral) (a) and average (functional) (b) model in boost operation

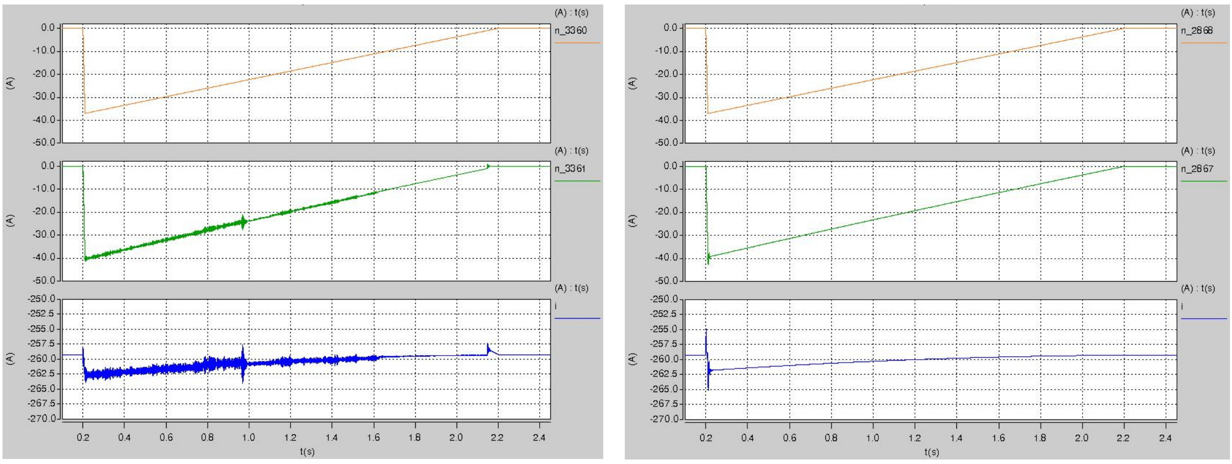

(a) (b)

Fig. 10: From top to bottom: transient current, converter output current and main generator current for switching (behavioral) (a) and average (functional) (b) model in buck operation

The operation of the DWHR converter for a load change can be seen in fig. 11, both for the switching and the average model. The consistency of the average model can be verified, thus it can be used for the analysis of the overall waste heat recovery system.

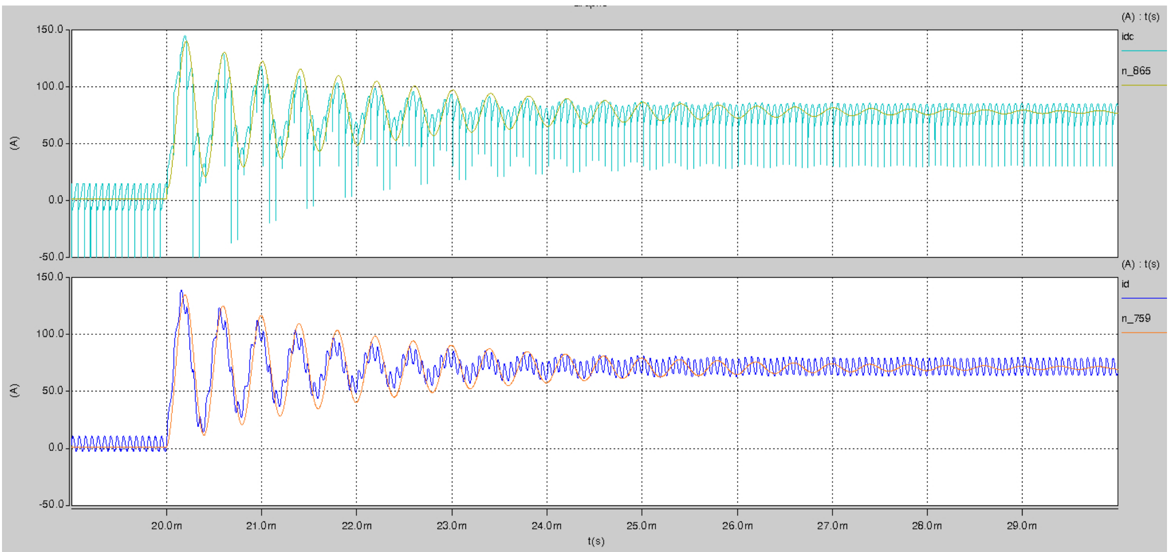

Fig. 11: Comparison between average (functional) and switching (behavioral) models. Output currents

Table I shows the comparison of time needed for the switching and the average models. Because of the switching phenomena of the semiconductor devices that have to be simulated, the simulation time step needs to be a lot smaller than the switching frequency, increasing so the simulation time needed. Since for the average models, the fundamental models of the devices are simpler, the simulation time is decreased. Moreover, the time step can be higher, as it is limited only by the resonant frequencies of the passive components. Therefore, the simulation time is decreased even more.

Finally, the operation of the full system, with both converters working together, is presented in fig. 12 via the use of the developed average models. When there is a fast transient load, the bidirectional buck/boost converter operates compensating the load current, whereas when there is a step load change the current is gradually provided by the DWHR converter. During the gradual change of DWHR reference the remaining current is again provided by the bidirectional converter. The DWHR converter also operates slightly during a fast transient load, since it can't rapidly distinguish if this is a step load. However this current is also compensated by the bidirectional converter as well. As it can be seen, the current provided by the main generator is effectively limited.

Table I: Simulation times for behavioral vs average models

	Behavioral model (time step=100ns)	Average model (time step=100ns)	Average model (time step=10us)
SWHR Current profile 1(fig. 9)	593s	445s	5.0s
SWHR Current profile 2 (fig 10)	2730s	1890s	24.2s
DWHR Current profile 1 (fig. 11)	85.4s	79s	0.93s

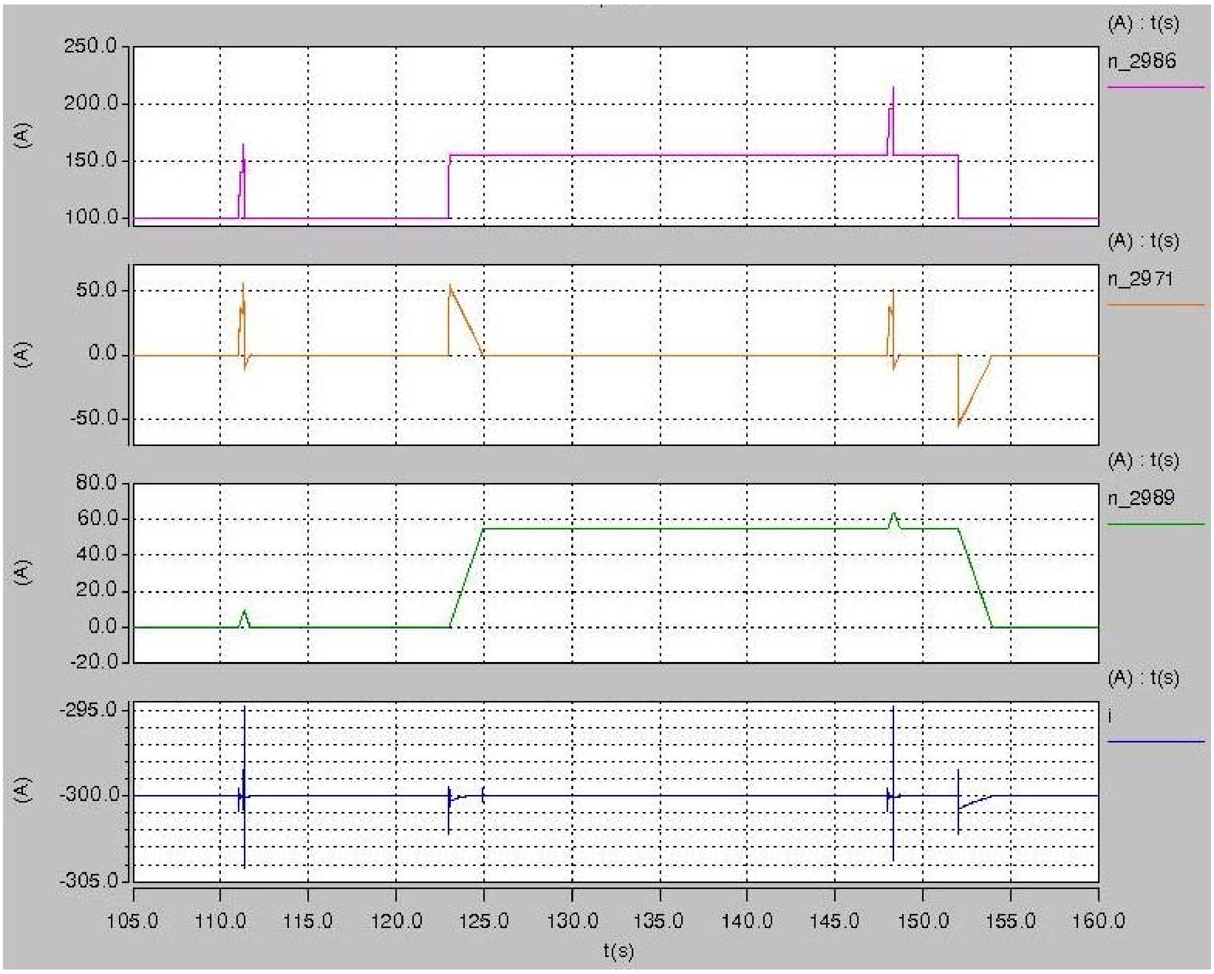

Fig. 12: From top to bottom: Transient load current, bidirectional converter output current, DWHR converter output current and main generator output current

Conclusion

In this paper, the operation of two waste heat energy recovery solutions has been presented, suitable for use in helicopters. Those systems take advantage of the combustion engine power losses in the form of exhaust gases heat and inject the recovered energy back in to the helicopter dc electrical supply system. Since before testing in a real helicopter, extensive simulations, in order to examine the

 ISBN: 978-90-75815-17-7 and 978-1-4799-0114-2

feasibility and the control strategy, have to be run, average models for the converters used have been developed so as to decrease the complexity and the simulation time. The simulation results presented show the validation of the average models provided as well as the control strategy employed.

References

[1] J. A. Rosero, J. A. Ortega, E. Aldabas, L. Romeral, "Moving towards a more electric aircraft," *IEEE Aerospace and Electronic Systems Magazine,* vol. 22, no. 3, pp. 3-9, April 2007.

[2] G. C. Christidis, I. Ch. Karatzaferis, I. Perpinias et al., "Innovative Waste Heat Recovery Systems in Rotorcrafts", *International Conference on Electrical Systems for Aircraft, Railway and Ship Propulsion (ESARS'12)*, 16-18 Oct. 2012.

[3] W. Chih, "Analysis of waste heat thermoelectric generators," *Applied Thermal Engineering,* vol. 16, no. 1, pp. 63-69, January 1996.

[4] D. Pavel, S. Lubos, "The energy storage system with supercapacitor for public transport," *IEEE Vehicle Power and Propulsion Conference,* 7-10 September 2009, pp. 1826-1830.

[5] A. Rufer, P. Barrade, "A supercapacitor-based energy storage system for elevators with soft commutated interface," *Record of the 2001 IEEE Industry Applications Conference,* 30 September - 4 October 2001, vol. 2, pp. 1413-1418.

[6] Y. S. Lee, "A systematic and unified approach to modeling switches in switch-mode power supplies", *IEEE Transactions on Industrial Electronics*, vol. IE-32, pp. 445-448, November 1985.

[7] M. K. Kazimierczuk, *Pulse-Width Modulated DC-DC Converters,* J. Wiley & Sons Inc., 2008.

[8] R. Tymerski and V. Vorperian, "Generation, classification, and analysis of switched-mode dc-to-dc converters by use of converter cell", *Proceedings of IEEE INTELEC'86*, October 1986, pp. 181-195.

[9] G. W. Wester, R. D. Middlebrook, Low-frequency characterization of switched dc-to-dc converters. *IEEE Transactions on Aerospace and Electronic Systems*, vol. AES-9, pp. 376-385, May 1973.

[10] R. D. Middlebrook and S. Cuk, "A general unified approach to modeling switching-converter power stages", *International Journal of Electronics*, vol. 42, no. 6, pp. 521-550, June 1977.

[11] W. M. Polivka, P. R. K. Chetty, and R. D. Middlebrook, "State-space average modeling of converters with parasitics and storage time modulation", *IEEE Power Electronics Specialists Conference Record,* 1980, pp. 119-143.

[12] N. Mohan, T. Undeland, W. Robbins, *Power Electronics Converters, Applications and Design*, J. Wiley & Sons, Inc., 1995.

[13] S. Chiniforoosh, "Averaged-circuit modeling of line-commutated rectifiers for transient simulation programs", ISCAS Proceedings of 2010 IEEE International Symposium on Circuits and Systems, May 2010, pp. 2318–2321.

[14] I. Jadric, D. Borojevic, and M. Jadric, "Modeling and control of a synchronous generator with an active DC load", *IEEE Transactions on Power Electronics*, vol. 15, no. 2, pp. 303-311, March 2000.

[15] H. Atighechi, "Approximate dynamic average-value model for controlled line-commuted converters, *24th Canadian Conference on Electrical and Computer Engineering*, 2011, pp. 966-970.

[16] M. Sautreuil, "Une nouvelle approche pour l'intégration des systèmes de generation aéronautique", PhD thesis, Universite Joseph Fourier, Nov. 2009.

[17] I. Laird, H. Lovatt, N. Savvides, D. Lu, V. G. Agelidis, "Comparative study of maximum power point tracking algorithms for thermoelectric generators", *Australasian Universities Power Engineering Conference (AUPEC '98),* 14-17 December 2008, pp. 1-6.

[18] Synopsis. Inc, SaberRD Quick Start Guide, Version F-2011.09, September 2011.

 ISBN: 978-90-75815-17-7 and 978-1-4799-0114-2